Sensor materials

Printed, Flexible, Ionic Liquid-Based Hydrogen Sensor via Aerosol Jet Printing of Nanomaterials

Huigang Wang[1], Xiaojun Liu[2], Yuhui Fang[3], Xiangqun Zeng[2], and Changyong (Chase) Cao[1,4*]

[1]*Department of Mechanical and Aerospace Engineering, Case Western Reserve University, Cleveland, OH 44106 USA*
[2]*Department of Chemistry, Oakland University, Rochester, MI 48309 USA*
[3]*4D Maker LLC, Okemos, MI 48864 USA*
[4]*Advanced Platform Technology (APT) Center, Louis Stokes Cleveland VA Medical Center, Cleveland, OH 44106 USA*
[*]*Member, IEEE*

Manuscript received 22 April 2023; accepted 1 May 2023. Date of publication 3 May 2023; date of current version 22 May 2023.

Abstract—Low-cost, high-performance hydrogen sensors are highly demanded in hydrogen leakage detection. To increase the sensitivity and reliability of the hydrogen sensor, an ionic liquid (IL)-based electrochemical gas sensor is fabricated with bimetallic Platinum–Nickel (Pt-Ni) nanoparticles (NPs) with aerosol jet printing technology for continuous monitoring of hydrogen concentration. The Pt-Ni NPs covering the top surface of the metal electrodes can accelerate the catalysis and expand the sensing surface area. When hydrogen gas is sensed at room temperature, the uniquely reversible and rapid redox reactions of hydrogen at the IL/Pt electrode interface, thereby creating continuous measurement capability in a real-time manner with little signal drift. The full coverage of the sensor electrodes will increase the robustness and accuracy of the device. The fabricated sensors demonstrate excellent analytical sensing performance, reaching a limit of detection up to 19.3 ppm. The device takes advantage of an easy fabrication process, simple structure, high sensing response, and low cost, providing a promise for hydrogen sensing at room temperatures.

Index Terms—Sensor materials, aerosol jet printing, flexible electronics, hydrogen sensors, nanomaterials, printed sensors.

I. INTRODUCTION

Hydrogen is the most important molecule for energy and has been widely used in many applications, from aerospace and chemicals to fuel cells and satellite power supplies. Although hydrogen is not toxic, it is highly flammable and dangerous because when hydrogen is mixed even in small amounts with ambient air, ignition/explosion can occur at a volumetric ratio of hydrogen to air as low as 4% due to the oxygen in the air. Thus, monitoring hydrogen leaks is essential for the use of hydrogen in hydrogen production, storage, and transportation, as well as all hydrogen-related applications. Most current hydrogen sensors consist of hydrogen-sensitive coatings, such as Pt, Pt/Pd, and Pd/MOx [1], [2]. When the coating adsorbs or reacts with hydrogen, its properties, such as optical, thermoelectric, thermal conductivity, resistance, and electronic will change, which can be related to the variation of hydrogen concentrations [3], [4]. However, these hydrogen sensors suffer from the degradation of the sensor coating materials; thus, sensor performance varies with time, resulting in the failure to sense hydrogen continuously and reliably. Thus, it is highly demanded that new hydrogen sensors can exhibit accuracy, repeatability, and stability regarding confounding factors, such as temperature variations in a range of ambient environments. It is also important to reduce the fabrication cost and enhance its reliability for large-scale deployments in broad applications.

Electrochemical (EC) sensors have been demonstrated as one of the most popular technologies that combine low-power consumption and analytical performance, enabling real-time measurement, high sensitivity, and selectivity at a relatively low cost. They are used for the measurement of H_2, CO, CO_2, NO_2, SO_2, and O_2 gases [5], [6], [7]. EC sensors rely on the measurements of the properties of the electrode and/or electrolyte as they interact with the analyte. Liquid electrolytes suffer from volatilities in ambient conditions and have limited specificity, service life, operating temperature range, and electrical potential range. As a result, solid electrolytes started to be used for EC gas sensors. However, solid electrolytes have low conductivity and often need high power to drive sensing reactions, e.g., the solid electrolytes in gas sensors operate at high temperatures, which can be hazardous for detecting explosive hydrogen gas, especially in harsh and explosive conditions.

To address these issues, ionic liquids (ILs) have been employed as solvents and electrolytes for fabricating sensors to provide an optimal solution to gas monitoring [8], [9]. ILs containing organic cations or anions is in a liquid state at room temperature but has negligible vapor pressure and is chemically and thermally stable at high temperatures (e.g., 200 °C). These characteristics overcome the problem of aging and poisoning of the sensing materials, allow the use of the sensor directly with ambient sampling conditions, and reduce the sensor hazards associated with flash points and flammability. In addition, ILs are electrically conductive and have a wide, stable potential window that enables the sensitive and selective detection of many gaseous analytes due to their unique EC sensing reactions in nonaqueous ILs that are not possible in conventional solvents [10], [11]. Thus, ILs are considered promising materials to produce new miniaturized, low-cost gas sensors that meet the demanding requirements for their uses in real-world applications [12], [13].

In this letter, we report a new flexible IL-based amperometric hydrogen sensor using aerosol jet printing of the Pt-Ni nanoparticles (NPs) on the printed gold electrodes. 1-butyl-1-methylpyrrolidinium bis(trifluoromethylsulfonyl)imide ($BmpyNTf_2$) serves as the electrolyte, enabling the uniquely reversible and rapid redox reactions of hydrogen at the IL/Pt electrode interface, thereby creating continuous

Corresponding author: Changyong (Chase) Cao (e-mail: ccao@case.edu)
Associate Editor: A. S. Dahiya. *(H. Wang and X. Liu contributed equally to this work.)*
Digital Object Identifier 10.1109/LSENS.2023.3272779

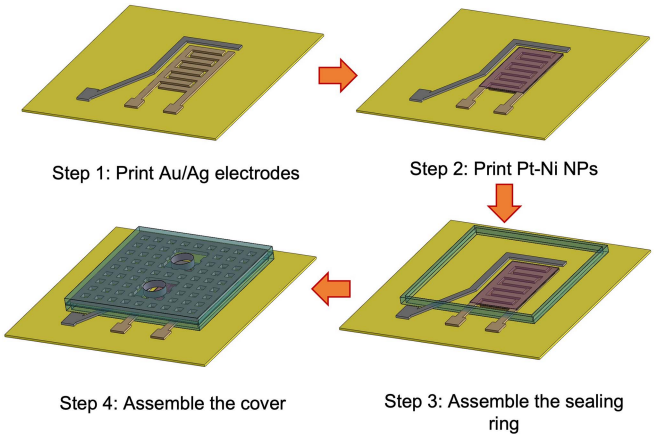

Fig. 1. Fabrication process of the hydrogen gas sensor with Pt-Ni NPs.

measurement capability in a real-time manner with little signal drift. Our innovative H_2 sensor addresses the issues of signal drift and cross sensitivities and provides highly reliable continuous hydrogen sensing with high sensitivity and selectivity. Furthermore, the printing technology significantly increases the interaction between the sensing NPs and the printed electrodes and reduces the fabrication cost and complexity.

II. FABRICATION

A. Printed Electrodes and Sensing Materials

Fig. 1 illustrates the fabrication process of the hydrogen sensor on a polyimide (Kapton) substrate. To use less printer ink and reduce the cost of the sensor, we utilized an aerosol jet printer (Nanojet Aerosol Printer, IDS Inc., USA) to fabricate the printed hydrogen sensors [14]. Gold NP ink (25wt%, UTDAu25TE, UT Dots LLC, USA) was used for the printing work. After optimization of the printing process, we selected the following printing parameters to fabricate high-resolution, high-quality conductive electrodes: carrier flow 9 sccm, sheath flow 60 sccm, printing speed 2 mm/s, atomization power 40 V, and platen temperature 25 °C. The diameter of the printer nozzle is 150 μm. The size of the printed sensor pattern is only about 2 cm × 2 cm. The printed electrodes were further thermally annealed in an oven at 280 °C for 30 min to improve the electrical conductivity.

The reference electrode of the sensor was also printed with silver NP-based inks (25wt%, Novacentrix LLC, USA) to reduce the drift of the sensor. The printing parameters for Ag (25wt%, Novacentrix, USA) were carrier flow 15 sccm, sheath flow 55 sccm, printing speed 2 mm/s, atomization power 41 V, and a platen temperature of 25 °C.

The sensing layer from the synthesized Pt-Ni NPs was printed on top of the working electrode (WE) and counter electrodes. The printing parameters for the Pt-Ni ink with a 150 μm nozzle were: carrier flow 22 sccm, sheath flow 49 sccm, printing speed 2 mm/s, atomization power 45 V, and platen temperature 25 °C. After printing, the sample was sintered in the oven at 150 °C for 20 min. Pt-Ni alloy NPs were synthesized by a simple, novel solvothermal method in which dimethylformamide and alcohol functioned as solvents and reductants [15]. The Pt-Ni alloy NPs supported on carbon black (Pt-Ni/C) were used as electrode materials that were fabricated in a planar miniaturized EC sensor device (see Fig. 2).

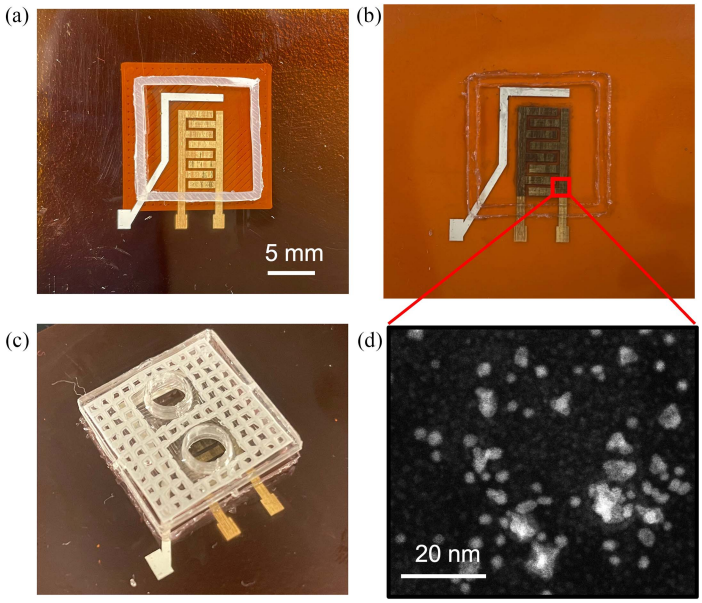

Fig. 2. Printed H_2 sensor prototype. (a) Printed gold and silver electrodes on a Kapton film. (b) Thin layer of Pt-Ni NPs was printed on the Au/Ag electrode surface as a sensing catalyst. (c) Assembled H_2 sensor prototype. (d) TEM image of the small Pt-Ni NPs.

B. Encapsulation of the H_2 Sensor Prototype

To keep the IL electrolyte at the right position on top of the electrodes and catalyst, we fabricated a square-shaped wall [see Fig. 2(a)] made of PDMS (Polydimethylsiloxane) and bonded it to the surface of the substrate of the printed sensor. An encapsulation box was 3-D printed with polylactide (PLA), and the dimension is 25 mm × 25 mm × 5 mm. The cured sensor was fixed in the encapsulation box by gluing the substrate with the internal surface of the box. Finally, a thin layer of IL electrolyte (∼1 mm thick) was cast on top of the interdigitated Pt-Ni electrodes to form a workable IL-H_2 sensor. A top cover sheet made of PLA mesh reinforced PDMS with inlet and outlet holes was finally bonded with the walls (see Fig. 2c). The H_2 sensing performance of the sensor devices was then tested in a controlled environment.

C. Device Testing

The EC measurements were conducted using a Versa STAT MC potentiostat (Princeton Applied Research, USA) with a three-electrode sensor device at room temperature. For cyclic voltammetry (CV) testing, N_2 (or H_2) was purged into the gas sensor chamber for at least 0.5 h) to saturate the electrolyte, followed by the CV measurements carried out in N_2 or H_2-saturated electrolytes between −0.2 and +0.8 V at a scan rate of 20 mV/s. Electrochemical impedance spectroscopy (EIS) was performed at open-circuit potential with a frequency range of 10^{-2}–10^5 Hz and an ac voltage amplitude of 5 mV [15]. Chronoamperometry (CA) measurements were conducted by setting the WE potential based on the oxidation peak potential from the CV results at 0.45 V. In the CA measurement, the background gas (N_2) was introduced into the sensor device for 300 s. After the background current decayed to a stable value, gaseous analyte (H_2) at a constant concentration was blown into the chamber for 300 s, and the steady-state current was collected as the sensing signal. All experiments were conducted at room temperature (25 ± 3 °C, 60 ± 5% RH) and atmospheric pressure.

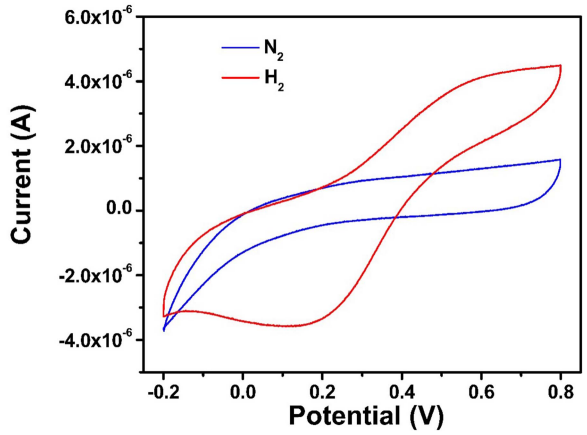

Fig. 3. CV of the device in N_2 (blue) and H_2 (red) saturated Bmpy NTf_2.

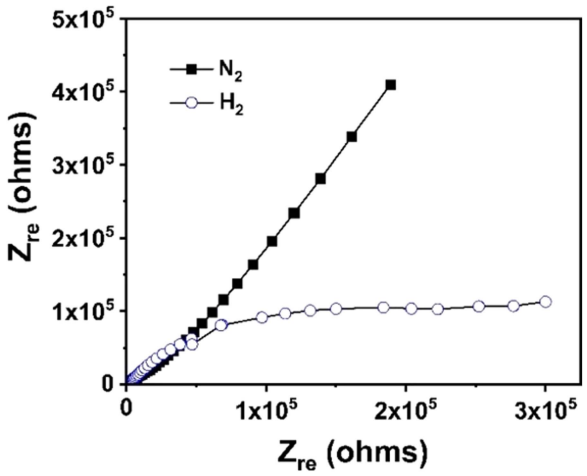

Fig. 4. EIS of the device in N_2 (black square) and H_2 (while circle) saturated $BmpyNTf_2$.

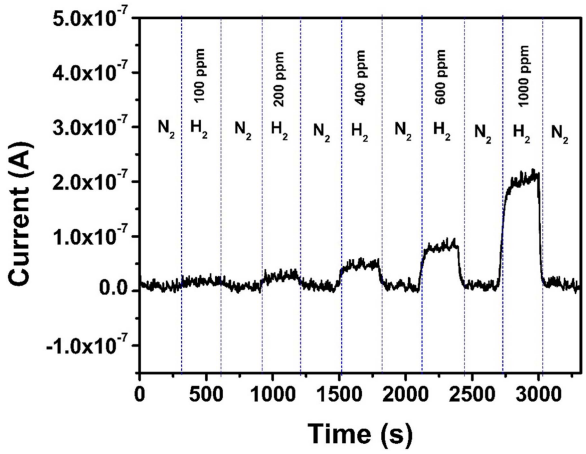

Fig. 5. CA of the device with the concentration of H_2 ranging from 100–1000 ppm in $BmpyNTf_2$ IL.

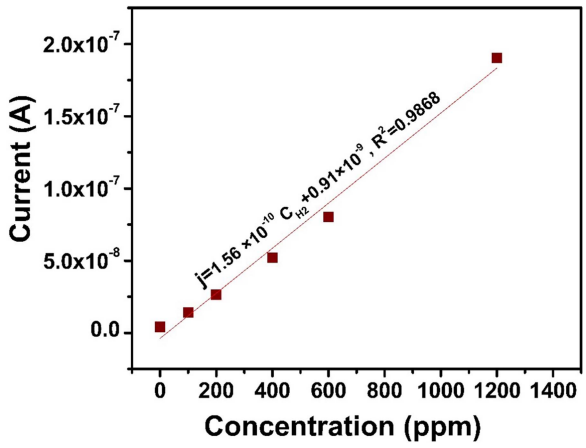

Fig. 6. Calibration curve of the sensor device: response current versus H_2 concentration.

III. RESULTS AND DISCUSSION

Figs. 3 and 4 present the CV and EIS of printed H_2 sensors in N_2 (blue) and H_2 (red) saturated Bmpy NTf_2, respectively. It is evident that in the N_2-saturated IL, no oxidation–reduction peaks were observed in the voltammogram within the potential window of 0–0.8 V, showing only a normal double-layer EC process. In contrast, in the H_2-saturated IL, obvious hydrogen oxidation peaks were observed during the anodic potential scan, and proton reduction peaks were observed during the cathodic potential scan.

The redox reaction of hydrogen gas is considered as the sensing mechanism of our sensor and can be represented by the following equations at anode and cathode. At the anode: Hydrogen gas is oxidized to hydrogen ions and the reaction equations are listed as follows:

$$H_2 + 2Pt \rightarrow 2Pt - H\,(ad) \tag{1}$$

$$Pt - H\,(ad) + A^- \rightarrow Pt + HA + e \tag{2}$$

where A is an anion in the electrolyte. At the cathode: Hydrogen ions are reduced to hydrogen atoms, and the process can be expressed as follows:

$$2HA + 2e \rightarrow H_2 + 2A^-. \tag{3}$$

Furthermore, it can be seen from Fig. 5 that CV comparison in N_2 and H_2 saturated $BmpyNTf_2$ indicates that the sensor has good sensitivity to hydrogen gas.

EC impedance testing was further used to study the EC process of the sensor. From the Nyquist plot in Fig. 4, in the low-frequency region, the sensor with the N_2-saturated IL exhibits a significant double-layer EC process, while in the H_2-saturated IL, there is a clear electron transfer process at the electrode-IL interface, indicating that the sensor is sensitive to hydrogen gas.

As shown in Fig. 5, Pt-Ni alloys nanocrystals exhibit good responsibility for hydrogen gas. As the concentration increases, the sensor's response current also increases. To better understand the relationship between hydrogen concentration and response current, we have constructed a calibration curve of the response current versus hydrogen concentration. Based on the calibration curve shown in Fig. 6, the current response of the sensor device showed excellent linear relation with the exposed hydrogen gas concentration, achieving a much lower LOD of 19.3 ppm. The obtained results in our work were compared with the IL-based EC H_2 sensors reported in the literature (see Table 1).

In Fig. 7, the repeatability test of the current sensor is demonstrated by subjecting it to sequential exposures of H_2 gas and comparing the mean output of all three exposures. The results show that the sensor exhibits a high level of repeatability, with typically less than 2.5%

TABLE 1. Comparison of Our IL-Based EC H_2 Sensors With Others Reported in the Literature

Gas	RTIL(s)	Electrode	Concentration	Ref.
H_2	[C_4mim]Cl	Pd deposited on carbon	1%–5%	[16]
H_2	[Bmpy][NTf_2]	Clark-type sensor with polycrystalline Pt gauze.	0.05%–1.25%	[17]
H_2	[Emim][NTf2]	Pt, porous Pt and GC	10%–100%	[18]
H_2	[Emim][NTf_2]	Pt, Au, and Au microchannel electrodes, modified with Pt NPs	10%–100%	[19]
H_2	Bmpy[NTf_2]	Pt-Ni/C	500–6250 ppm	[15]
H_2	Bmpy[NTf_2]	Pt-Ni/C	100–1000 ppm	This work

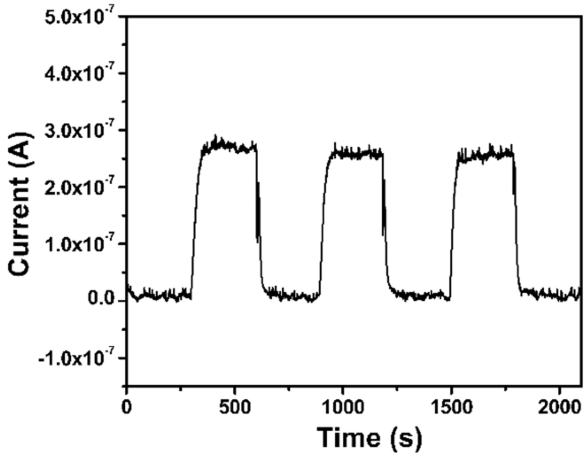

Fig. 7. Sensor signal after two months since last-time test upon exposure to 1000 ppm of H_2 gas at room temperature.

variation compared to the mean output. Furthermore, the stability of the sensor is confirmed by conducting the measurement in Fig. 7 again after two months at room temperature, indicating its excellent performance. The sensor's selectivity was evaluated in relation to various interference gases, such as Air, SO_2, CO, CH_4, O_2, and CO_2, at a concentration of 5000 ppm, as compared to 500 ppm of H_2 at the operating potential for hydrogen oxidation. The sensor demonstrates a significantly higher response signal to 500 ppm of H_2, surpassing the response to other gases, implying its exceptional selectivity toward H_2.

IV. CONCLUSION

In this letter, we have presented a new flexible IL-based hydrogen sensor using aerosol jet printing of the Pt-Ni NPs on printed electrodes. The uniquely reversible and rapid redox reactions of hydrogen at the IL/Pt electrode interface and the increased surface area from smaller NPs and printed electrodes addresses the issues of signal drift and cross sensitivities, and provides highly reliable continuous hydrogen sensing with high sensitivity and selectivity. The printing technology will also significantly reduce the fabrication cost and complexity.

ACKNOWLEDGMENT

This work was supported in part by the U.S. Department of Energy under Grant DE-SC0021753, in part by the USDA-NIFA under Grant 2021-67021-33998, and in part by the Case Western Reserve University.

REFERENCES

[1] M. P. Suh et al., "Hydrogen storage in metal-organic frameworks," *Chem. Rev.*, vol. 112, no. 2, pp. 782–835, Feb. 2012.
[2] C. Ramesh et al., "An improved polymer electrolyte-based amperometric hydrogen sensor," *J. Solid State Electrochemistry*, vol. 7, no. 8, pp. 511–516, Aug. 2003.
[3] I. Lundstrom et al., "Twenty-five years of field effect gas sensor research in linkoping," *Sensors Actuators B-Chem.*, vol. 121, no. 1, pp. 247–262, Jan. 2007.
[4] J. Hu et al., "Amperometric sensor for the detection of hydrogen stable isotopes based on Pt nanoparticles confined within single-walled carbon nanotubes (SWNTs)," *Sensors Actuators B: Chem.*, vol. 356, Apr. 2022, Art. no. 131344.
[5] R. Knake et al., "Amperometric detection of gaseous formaldehydein the ppb range," *Electroanalysis*, vol. 13, no. 8/9, pp. 631–634, 2001.
[6] R. Knake et al., "A direct comparison of amperometric gas sensors with gas-diffusion and ion-exchange membrane based electrodes," *Analyst*, vol. 127, no. 1, pp. 114–118, Jan. 2002.
[7] G. Korotcenkov et al., "Review of electrochemical hydrogen sensors," *Chem. Rev.*, vol. 109, no. 3, pp. 1402–1433, Mar. 2009.
[8] Z. Wang et al., "Methane-oxygen electrochemical coupling in an ionic liquid: A robust sensor for simultaneous quantification," *Analyst*, vol. 139, no. 20, pp. 5140–5147, 2014.
[9] X. Q. Zeng et al., "Glycosylated conductive polymer: A multimodal biointerface for studying carbohydrate-protein interactions," *Accounts Chem. Res.*, vol. 49, no. 9, pp. 1624–1633, Sep. 2016.
[10] A. Rehman and X. Zeng, "Methods and approaches of utilizing ionic liquids as gas sensing materials," *RSC Adv.*, vol. 5, no. 72, pp. 58371–58392, 2015.
[11] Z. Wang et al., "Methane recognition and quantification by differential capacitance at the hydrophobic ionic liquid-electrified metal electrode interface," *J. Electrochem. Soc.*, vol. 160, no. 6, pp. B83–B89, Jan. 2013.
[12] E. S. Forzani et al., "A hybrid electrochemical-colorimetric sensing platform for detection of explosives," *J. Amer. Chem. Soc.*, vol. 131, no. 4, pp. 1390–1391, Feb. 2009.
[13] Y. Liu et al., "Preparation of porous aminopropylsilsesquioxane by a nonhydrolytic sol-gel method in ionic liquid solvent," *Langmuir*, vol. 21, no. 4, pp. 1618–1622, Feb. 2005.
[14] Y. Zhou et al., "4D printing of stretchable supercapacitors via hybrid composite materials," *Adv. Mater. Technol.*, vol. 6, no. 1, Jan. 2021, Art. no. 2001055.
[15] X. Liu et al., "Platinum–nickel bimetallic nanosphere–ionic liquid interface for electrochemical oxygen and hydrogen sensing," *ACS Appl. Nano Mater.*, vol. 2, no. 5, pp. 2958–2968, May 2019.
[16] E. Jayanthi et al., "Sensing behavior of room temperature amperometric H_2 sensor with Pd electrodeposited from ionic liquid electrolyte as sensing electrode," *J. Electrochem. Soc.*, vol. 164, no. 8, 2017, Art. no. H5210.
[17] Y. Tang et al., "Continuous amperometric hydrogen gas sensing in ionic liquids," *Analyst*, vol. 143, no. 17, pp. 4136–4146, 2018.
[18] G. Hussain et al., "Macroporous platinum electrodes for hydrogen oxidation in ionic liquids," *Electrochemistry Commun.*, vol. 86, pp. 43–47, 2018.
[19] G. Hussain et al., "Fast responding hydrogen gas sensors using platinum nanoparticle modified microchannels and ionic liquids," *Analytica Chimica Acta*, vol. 1072, pp. 35–45, 2019.